Thoracic Biomechanical Responses of Small Female PMHS in a Simplified Side Impact Condition

Srinivas Anantharamakrishnan[1], Andrew Kemper[2], Gretchen H. Baker[1], Allison J. Guettler[1], Heather Rhule[2], Yun-Seok Kang[1], Amanda M. Agnew[1]

[1] Injury Biomechanics Research Center, The Ohio State University, USA

[2] Vehicle Research and Test Center, National Highway Traffic Safety Administration, USA

ABSTRACT

Biomechanical response targets for the thorax have largely focused on the 50th percentile male, limiting their relevance for smaller females. Previous studies have provided side impact female PMHS data from either oversimplified or realistic boundary conditions. This study aimed to generate thoracic biomechanical responses of small female PMHS in a simplified side impact condition with realistic components and compare responses between two input energy levels. Twelve small female PMHS were seated on a simplified seat with FMVSS No. 213a seat foam and fabric and impacted once on the left thorax with either a 14.0 kg (low energy) or 23.7 kg (high energy) pneumatic impactor at 4.5 m/s. A rectangular impactor face (22.9 × 25.4 cm) covered with FMVSS No. 213a armrest foam simulated an intruding door panel. Thoracic deflection was measured using a chestband. Inertially compensated force was recorded via a load cell. Spinal kinematics were captured using six-degree-of-freedom motion blocks. Biomechanical responses were compared between groups using two sample t-tests. The high-energy group exhibited significantly higher peak forces (2.5 vs 1.9 kN, p=0.0001), greater thoracic deflections (41.0 vs 33.9 mm, p=0.016), and increased deformation energy (91.6 vs 61.0 J, p=0.0001). Effective stiffness did not differ significantly between groups (p=0.734). Energy loss increased with impact severity (66.2 vs 56.7 %, p=0.020). Kinematic responses also increased with increased input energy. Peak y-accelerations were significantly greater at T4 in the high energy group (p=0.049). The sternum exhibited significantly greater peak z-angular velocity in the high-energy group (p=0.038). Mean BRSS of the F-D corridors between groups was 0.93. In summary, these findings provide essential biomechanical data and establish an important foundation for developing improved testing conditions and advancing the evaluation of female HBMs and ATDs in side impact scenarios.

This paper is a student paper from the 21st Injury Biomechanics Symposium and is published in a special issue of SAE International Journal of Transportation Safety.
It is preliminary work, has not been peer reviewed, and should not be cited because it is a work in progress.

INTRODUCTION

Females may be at a higher risk of thoracic injuries in nearside side impact crashes compared to males (Noh et al., 2022, Bose et al., 2011). Brumbelow and Jermakian (2022) showed that much of the observed sex differences in thoracic injury risk can be attributed to variations in crash severity, vehicle type, and impact configuration. Furthermore, the striking vehicle type significantly influences the severity of lateral loading experienced by the struck occupant (Brumbelow et al., 2015) and significantly influences injury outcomes, with impacts involving pickup trucks and SUVs associated with higher injury rates compared to car-to-car impacts due to their greater mass and elevated ride height (Prasad et al., 2015). Injury outcomes for female occupants are often governed by multiple interacting factors, including vehicle mass, crash severity, and occupant characteristics (Dalmotas et al., 2024, Craig et al., 2026). Collectively, these findings highlight the complexity of real-world crash conditions and the difficulty in isolating the effects of individual variables such as impact energy.

A previous experimental study by Nusholtz et al. (1983) investigated thoracic biomechanical response of post-mortem human subjects (PMHS) using variations in impactor energy by changing the impactor mass. They demonstrated that increased impact energy results in greater thoracic deformation, higher force, and increased likelihood of rib fractures. However, the study primarily focused on injury outcomes and peak response metrics, with limited characterization of full force-deflection corridors and a lack of female data. Additional challenges with instrumentation and measurement techniques at the time restricted detailed assessment of force-deflection responses and specific fracture timing.

Despite the documented vulnerability of female occupants in side impact crashes, female-specific biomechanical response data remain uncommon in the literature. Foundational thoracic response corridors have provided essential data for side impact anthropomorphic test device (ATD) development and validation, but these were generated predominantly from scaling mid-size male PMHS responses (Shaw et al., 2006, Rhule et al., 2011).

Agnew et al. (2024) tested small female PMHS under simplified boundary conditions and compared responses to scaled male data, but multiple impacts prevented injury outcome evaluation. Additionally, the absence of realistic boundary conditions limits the applicability of these data to real-world scenarios. Bolte et al. (2023) tested elderly small female PMHS under realistic vehicle conditions including a production seat, airbag, and seatbelt, better representing real-world crash environments. However, the complexity of this experimental setup makes it difficult to isolate individual factors governing thoracic response, identify injury mechanisms, and use the data for straightforward ATD and human body model (HBM) evaluation.

There remains a paucity of female PMHS thoracic response and injury data in experimental side impact studies, especially with realistic loading scenarios. Additionally, there is a limited understanding of how impact energy, representing the combined effect of impactor mass and velocity conditions, influences biomechanical responses. To address these gaps, the objective of

This paper is a student paper from the 21st Injury Biomechanics Symposium and is published in a special issue of SAE International Journal of Transportation Safety.
It is preliminary work, has not been peer reviewed, and should not be cited because it is a work in progress.

the current study was to generate thoracic biomechanical response data for small female PMHS in a simplified side impact condition with realistic components and make direct comparisons between two input energy levels.

METHODS

Experimental setup and test matrix

A simplified experimental setup was used to isolate the lateral thoracic response. The setup consisted of a rigid seat with FMVSS No. 213a seat foam (5.1 cm thick) and fabric covering the seat pan and back (Figure 1a), with the seatback angled at 18° from vertical and the seat pan at 15° from horizontal. PMHS were seated upright with no belt and were free to translate during impact. The upper extremities were raised and retracted posteriorly to minimize scapula interference. Since the arm can introduce variability into the thoracic response and injury outcomes (Kemper et al., 2008), it was a priority to ensure the humerus was not engaged with the impactor. A bra was used to position the breasts naturally and out of the direct load path (Baker et al., 2026). The impactor was positioned inferior to the axilla and superior to the pelvis to isolate the thoracic region. A rigid rectangular face (22.9 × 25.4 cm) covered with 6.3 cm thick FMVSS No. 213a armrest foam was used to simulate an intruding door panel (Figure 1b). Each PMHS was impacted once on the left thorax at a target velocity of 4.5 m/s. Six PMHS (1–6) were impacted with a 14.0 kg mass (low energy, target 139 J) and six PMHS (7–12) with a 23.7 kg mass (high energy, target 260 J) (Table 1). A five-axis load cell was mounted behind the impactor plate to measure impactor force, and accelerometers attached to the impactor plate were used to calculate velocity and perform inertial compensation for the impactor force. The in-position posture of each PMHS was documented by obtaining lateral X-rays. In addition, a 3D coordinate measurement device and laser line probe (Faro Technologies, Lake Mary, FL, USA) were used to scan (Figure 1c) and digitize 3D coordinates of bony landmarks and impactor locations prior to testing. The in-position seating posture of the PMHS is shown in (Figure 1d).

Table 1: Test Matrix

PMHS	Test Group	Impact Location	Target Velocity (m/s)	Impactor Shape and Size (cm)	Impactor Mass (kg)
1–6	Low Energy	Left Thorax	4.5	Rectangle (22.9 x 25.4)	14.0
7–12	High Energy	Left Thorax	4.5	Rectangle (22.9 x 25.4)	23.7

PMHS Characteristics & Instrumentation

Twelve small female PMHS were utilized in this study for which ethics approval from The Ohio State University Body Donation Program was obtained prior to testing. Computed tomography (CT) scans allowed for exclusion based on any pre-existing thoracic trauma. All

This paper is a student paper from the 21st Injury Biomechanics Symposium and is published in a special issue of SAE International Journal of Transportation Safety.
It is preliminary work, has not been peer reviewed, and should not be cited because it is a work in progress.

PMHS anthropometric characteristics (Irwin et al., 2002) were similar (Table 2) between the two test groups (two sample t-test, $p > 0.05$).

a) Seat and seat foam (FMVSS 213a)

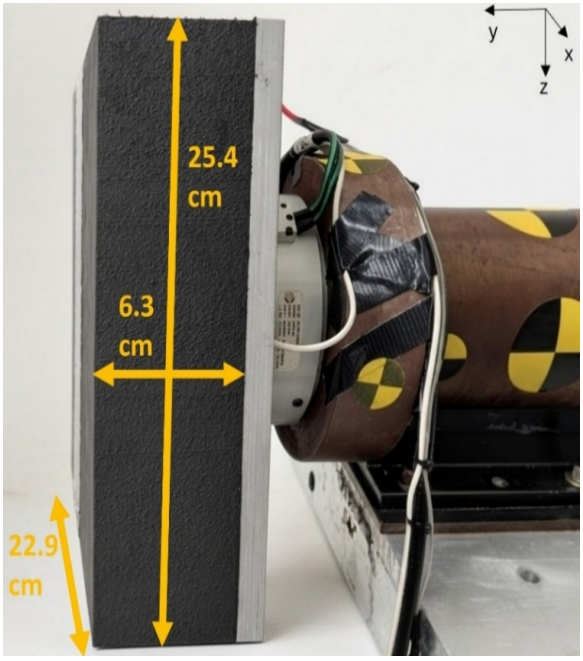

b) Impactor with armrest foam (FMVSS 213a)

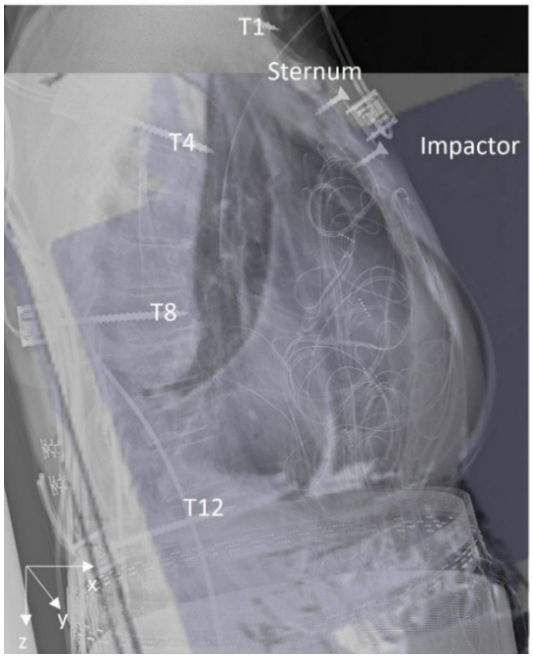

c) Faro scan and x-ray overlay showing impactor position

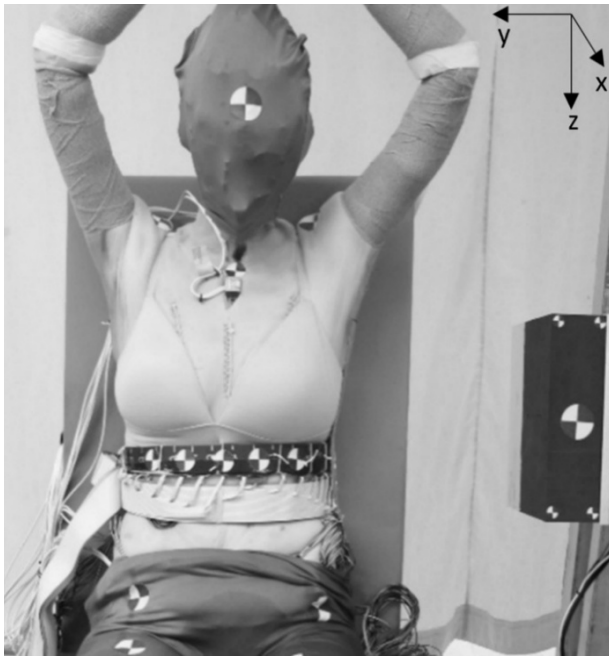

d) Initial PMHS seating posture and test set-up

Figure 1: Seat and impactor details with experimental setup

This paper is a student paper from the 21st Injury Biomechanics Symposium and is published in a special issue of SAE International Journal of Transportation Safety.
It is preliminary work, has not been peer reviewed, and should not be cited because it is a work in progress.

Table 2: PMHS Characteristics

	PMHS	Age (yrs)	Height (cm)	Weight (kg)	BMI	Lumbar aBMD (t-score)	Seated Height (cm)	Seated Shoulder Height (cm)
Low Energy	1	80	159.3	47.2	18.6	-1.4	84.4	63.7
	2	81	155.1	49.9	20.7	0.0	84.6	63.1
	3	79	154.8	44.2	18.4	-1.3	81.7	60.4
	4	46	158.7	40.1	15.9	-2.4	87.6	64.4
	5	59	166.0	50.8	18.4	-0.5	90.2	64.6
	6	68	161.5	58.5	22.4	-1.7	86.7	65.4
	Mean	**68.8**	**159.2**	**48.5**	**19.1**	**-1.2**	**85.9**	**63.6**
	SD	**14.1**	**4.2**	**6.3**	**2.2**	**0.8**	**2.9**	**1.8**
	Target	**-**	**151.0**	**46.7**	**20.5**	**-**	**81.2**	**-**
High Energy	7	86	152.4	56.2	24.2	-1.3	77.4	58.0
	8	64	157.5	54.9	22.1	-3.0	87.8	67.5
	9	72	158.8	43.5	17.2	-1.3	86.6	63.9
	10	82	167.6	40.8	15.0	0.2	84.8	62.9
	11	64	152.4	56.5	24.0	-1.7	81.1	60.6
	12	75	157.5	45.8	18.0	-0.2	85.3	62.5
	Mean	**73.8**	**157.7**	**49.6**	**20.1**	**-1.2**	**83.9**	**63.2**
	SD	**9.1**	**5.6**	**7.1**	**3.9**	**1.1**	**3.9**	**3.2**
	Target	**-**	**151.0**	**46.7**	**20.5**	**-**	**81.2**	**-**

Instrumentation was consistent with Agnew et al. (2024). A 59-Channel chestband (Model 8641 1-6, Humanetics, Plymouth, MI, USA) was circumferentially secured at the same level as the center of impactor, which corresponded to approximately the level of the xiphoid process and the bra band. The chestband was installed using 7 kg of tension and then sutured to the skin at approximately 5 cm intervals to ensure proper attachment. Spinal kinematics were measured using 6-degree-of-freedom motion blocks (6DX PRO, Diversified Technical Systems, Seal Beach, CA, USA) rigidly mounted to the posterior thoracic vertebrae at T1, T4, T8, and T12. An additional motion block was installed on the manubrium.

Data Acquisition & Analysis

All data channels were recorded at 20,000 Hz using a SLICE PRO (DTS, Seal Beach, CA, USA) data acquisition system, and three high-speed cameras captured frontal, frontal-oblique, and overhead views (Phantom VEO 710L & Miro 320s, AMETEK Inc., Wayne, NJ, USA) at 1,000 or 5,000 Hz. Except for the chestband, all channels were zeroed prior to impact to remove any pre-existing offset and filtered using CFC filters per SAE J211 guidelines. Load cell and impactor accelerometer data were filtered at CFC180. Impact velocity was obtained by numerically integrating the filtered accelerometer data. Input kinetic energy was calculated using the velocity

This paper is a student paper from the 21st Injury Biomechanics Symposium and is published in a special issue of SAE International Journal of Transportation Safety.
It is preliminary work, has not been peer reviewed, and should not be cited because it is a work in progress.

at impact and impactor mass. Inertial compensation was applied to get the thoracic force at contact. This was achieved by subtracting the product of impactor face mass of 2.5 kg which contained the mass of all components between the load cell and contact surface and included the impactor face plate and foam. This was then multiplied by the filtered ram accelerometer (CFC180) and then subtracted from the filtered load cell output (CFC180). Chestband data were processed using CrashStar software (v2.7) to generate thoracic contours throughout the impact. Thoracic deflection was quantified using the half lateral deflection method (Yoganandan et al., 2011), filtered at CFC600, and percent peak deflection was normalized by the initial chest breadth at the xiphoid process.

Deformation energy (DE) was calculated by integrating the force-deflection response of the thorax during impact as outlined in Moorhouse (2013).

$$DE = \int_0^{y_{\max}} F(t)dy(t) \quad \text{[Eq. 1]}$$

Where: DE = Deformation energy

F(t) = Force

die(t) = Deflection

$y_{\max}$ = Max deflection

The energy input-output relationship was quantified using the energy ratio, defined as the ratio of deformation energy to the initial kinetic energy. The energy loss is calculated as the remaining fraction of energy not recovered, expressed as a percentage.

Thoracic stiffness was quantified using an energy-based formulation derived from the experimentally measured force-deflection response. Thoracic response was approximated as linear elastic within the loading range, where the absorbed deformation energy is equivalent to the elastic potential energy of a spring.

$$DE = \frac{1}{2} k y_{max}^2 \quad \text{[Eq. 2]}$$

Where: k = Stiffness

Rearranging the elastic potential energy expression to solve for stiffness,

$$k = \frac{2DE}{y_{max}^2} \quad \text{[Eq. 3]}$$

Filtered acceleration and angular velocity data from the 6DX motion blocks were transformed into anatomical coordinate systems derived from CT-based segmentation (Mimics, Materialise NV) following the methods of Slykhouse et al. (2019).

This paper is a student paper from the 21st Injury Biomechanics Symposium and is published in a special issue of SAE International Journal of Transportation Safety.
It is preliminary work, has not been peer reviewed, and should not be cited because it is a work in progress.

Statistical Analysis

Peaks were compared between the two energy groups. Since normality was not assessed and sample sizes were small, both two-sample t-tests (p_T) and Mann-Whitney tests ($p_{M\text{-}W}$) were conducted to determine whether impact energy levels significantly influenced thoracic biomechanical response. These tests were performed using Minitab (Minitab version 17, LLC, State College, PA, USA). Significance was established *a priori* at $\alpha = 0.05$. 2D biomechanical response corridors were created by calculating the mean ± one standard deviation of the force and deflection time history curves (Shaw et al., 2006). No phase optimization was performed on the individual curves. BioRank System Scores (BRSS) were calculated using the methods outlined in Kang et al. (2023).

RESULTS

Biomechanical response summary

The two energy groups were intended to be tested at the same impact velocities (4.5 m/s) while varying the impactor mass to achieve different levels of input kinetic energy. The mean impact velocities achieved for each group are reported in Table 3. The coefficient of variation (CV) for the actual impact velocity in the low energy group was 2.6 % and the high energy group was 2.1 %, indicating high repeatability within each group. Kinetic energy was significantly greater in the high energy group (low energy group: 139.2 ± 7.4 J; high energy group: 260.3 ± 7.4 J; $p_T < 0.0001$; $p_{M\text{-}W} = 0.005$). This increased kinetic energy applied in the high energy group amplified the thoracic biomechanical responses as expected (Table 3). The high energy group exhibited significantly greater peak force (2566 N vs. 1997 N; $p_T < 0.0001$, $p_{M\text{-}W} = 0.005$), peak deflection (41.0 mm vs. 33.8 mm; $p_T = 0.016$, $p_{M\text{-}W} = 0.006$), percent peak deflection (15.7 % vs. 12.2 %; $p_T = 0.004$, $p_{M\text{-}W} = 0.005$), deformation energy (91.6 J vs. 61.0 J; $p_T < 0.0001$, $p_{M\text{-}W} = 0.005$), and energy loss (66.1 % vs. 56.6 %; $p_T = 0.020$, $p_{M\text{-}W} = 0.031$) compared to the low energy group . Despite these increases, effective thoracic stiffness was similar between groups (110.9 N/mm vs. 107.6 N/mm; p_T, $p_{M\text{-}W} > 0.05$).

This paper is a student paper from the 21st Injury Biomechanics Symposium and is published in a special issue of SAE International Journal of Transportation Safety.
It is preliminary work, has not been peer reviewed, and should not be cited because it is a work in progress.

Table 3: Low vs. High Energy Group Comparisons for Calculated Biomechanical Data

	Low Energy		High Energy		T-test p-value*	M-W test p-value*
	Mean ± SD	**Median**	**Mean ± SD**	**Median**		
Impact Velocity (m/s)	4.4 ± 0.1	4.4	4.7 ± 0.1	4.6	**0.005**	**0.020**
Kinetic Energy (J)	139.2 ± 7.4	137.4	260.3 ± 10.9	260.6	**<0.0001**	**0.005**
Peak Force (N)	1997.0 ± 128.0	2034.0	2566.0 ± 161.0	2588.0	**<0.0001**	**0.005**
Peak Deflection (mm)	33.8 ± 4.1	35.8	41.0 ± 4.3	40.7	**0.016**	**0.006**
Peak Deflection (%)	12.2 ± 1.1	12.7	15.7± 1.8	15.1	**0.004**	**0.005**
Deformation Energy (J)	61.0 ± 8.9	62.9	91.6 ± 6.8	93.8	**<0.0001**	**0.005**
Energy Loss (%)	56.6 ± 6.9	57.5	66.1 ± 3.1	64.5	**0.020**	**0.031**
Stiffness (N/mm)	107.6 ± 13.6	100.2	110.9 ± 18.7	108.1	0.734	1.000

*Bolded p-values are significant, M-W = Mann-Whitney (non-parametric) test

Peak kinematic responses were also evaluated between energy groups, and the results are summarized in Table 4. As expected, mean peak y-axis accelerations were greater in the high energy group, showing increased translational motion in the primary loading direction aligned with the impactor. However, this increase was only statistically significant between groups at T4 (p_T = 0.049, $p_{M\text{-}W}$ = 0.045). Angular velocity about the x-axis was not significantly different between groups at any spinal level ($p > 0.05$). Angular velocity about the z-axis was significantly greater in the high energy group at the sternum (p_T = 0.038, $p_{M\text{-}W}$ = 0.045) but not any of the spine levels.

This paper is a student paper from the 21st Injury Biomechanics Symposium and is published in a special issue of SAE International Journal of Transportation Safety.
It is preliminary work, has not been peer reviewed, and should not be cited because it is a work in progress.

Table 4: Low vs. High Energy Group Comparisons of Kinematic Data

	Peak Response	Low Energy		High Energy		T-test p-value*	M-W test p-value*
		Mean ± SD	Median	Mean ± SD	Median		
Sternum	Acceleration y (g)	21.3 ± 10.2	20.67	25.7 ± 8.1	26.4	0.419	0.471
	Angular Velocity x (deg/s)	-220.0 ± 131.0	-211.8	-277.0 ± 106.0	-250.4	0.430	0.471
	Angular Velocity z (deg/s)	572.0 ± 265.0	542.0	912.0 ± 219.0	885.0	**0.038**	**0.045**
T1	Acceleration y (g)	16.5 ± 3.7	14.9	21.4 ± 3.5	20.8	**0.046**	0.093
	Angular Velocity x (deg/s)	-448.0 ± 137.0	-423.0	-530.0 ± 162.0	-529.6	0.372	0.471
	Angular Velocity z (deg/s)	197.5 ± 91.9	207.9	129.0 ± 206.0	206.5	0.487	0.689
T4	Acceleration y (g)	18.2 ± 4.9	16.9	24.2 ± 4.2	23.8	**0.049**	**0.045**
	Angular Velocity x (deg/s)	-383.0 ± 116.0	-376.2	-372.0 ± 288.0	-347.8	0.933	0.810
	Angular Velocity z (deg/s)	-147.6 ± 95.1	-123.8	-249.0 ± 157.0	-219.8	0.214	0.298
T8	Acceleration y (g)	23.1 ± 5.0	21.2	32.5 ± 8.5	33.1	**0.048**	0.093
	Angular Velocity x (deg/s)	180.0 ± 127.0	135.8	314.9 ± 86.5	289.4	0.064	0.066
	Angular Velocity z (deg/s)	-352.0 ± 155.0	-383.6	-315.0 ± 294.0	-448.3	0.791	0.689
T12	Acceleration y (g)	27.9 ± 8.0	25.1	37.2 ± 18.0	28.7	0.292	0.378
	Angular Velocity x (deg/s)	563.0 ± 181.0	469.4	732 ± 265.0	720.1	0.233	0.575
	Angular Velocity z (deg/s)	246.0 ± 120.0	220.5	182.0 ± 116.0	166.4	0.371	0.471

***** Bolded p-values are significant, M-W = Mann-Whitney (non-parametric) test

This paper is a student paper from the 21st Injury Biomechanics Symposium and is published in a special issue of SAE International Journal of Transportation Safety.
It is preliminary work, has not been peer reviewed, and should not be cited because it is a work in progress.

Force-Deflection Response

Force-deflection corridors were developed for each energy group (Figure 2). The width of each corridor reflects PMHS variability within the groups. The low-energy group exhibits a relatively tighter corridor, indicating more consistent responses across PMHS whereas the high-energy group shows a broader corridor. This greater variability is mostly observed at the beginning of the corridor but decreases toward the later stages of the response as the curves converge and variability decreases. The BRSS values were calculated between 0 to 50 ms and are summarized in Table 5 with an overall mean BRSS between the groups of 0.93.

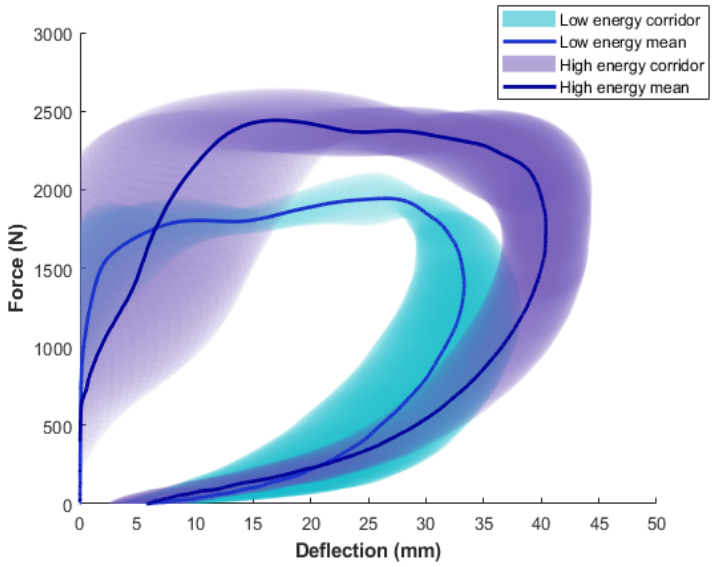

Figure 2: Force-deflection corridors of the low energy (cyan) and high energy group (violet)

Table 5: BRSS Between Input Energy Groups

Force-time			Deflection-time			F-D
Low vs High	**High vs Low**	**Mean**	**Low vs High**	**High vs Low**	**Mean**	**Mean BRSS**
0.58	1.75	1.16	0.47	0.94	0.70	0.93

This paper is a student paper from the 21st Injury Biomechanics Symposium and is published in a special issue of SAE International Journal of Transportation Safety.
It is preliminary work, has not been peer reviewed, and should not be cited because it is a work in progress.

DISCUSSION

This study successfully quantified thoracic biomechanical response in twelve small female PMHS under well-controlled side-impact conditions with realistic components. Aligning with frontal hub impact studies by Kroell et al. (1971, 1974), the results from this study confirm that increase in kinetic energy produces greater peak forces, chest deflections, and deformation energy as shown in Table 3. Effective thoracic stiffness did not differ significantly between groups ($p = 0.734$), suggesting that the intrinsic structural resistance of the thorax was not fundamentally altered by the change in impact energy. This is plausible given that structural stiffness shows the resistance of the thorax to deformation, that may remain relatively consistent across the range of energy levels tested, particularly when the increase in impactor mass was modest (factor of 1.69) and inter-subject variability in thoracic geometry, bone quality, and soft tissue distribution was inherently present within each group. Additionally, since stiffness was estimated using an energy-based formulation (Moorhouse, 2013), the proportional increases in both deformation energy and peak deflection with impact severity may have further contributed to the similarity in calculated stiffness between groups.

Force-deflection corridors (Figure 2) revealed that response variability differed across phases and between energy groups. During the loading phase, the high energy group showed greater variability reflected in the wider corridor. Beyond peak force, the low energy group showed greater deflection variability, potentially reflecting subject-specific differences in bone quality, BMI, geometry, or soft tissue distribution. The overall BRSS of 0.93 (0–50 ms) suggests globally similar response enveloped between energy conditions yet masks important regional differences. The elevated force-time BRSS (mean: 1.16) indicated that the force response of the high energy group falls outside one standard deviation of the low energy group corridor, reflecting a greater force corridor in the high energy group.

Agnew et al. (2024) performed lateral impact tests for four small female PMHS using a rectangular rigid impactor face (12.5 × 27.5 cm) with a mass of 14 kg at an impact velocity of 4.5 m/s. These conditions allowed for a direct comparison to the current study's low energy group that used a larger impactor face (22.9 × 25.4 cm) with foam padding but the same impactor mass and impact velocity. Agnew et al. (2024) did not use a seatback in their tests but rather positioned the PMHS with the spine vertical in a “free back” condition. Additionally, force-time and deflection-time phase optimization was performed, shifting the final mean responses such that time zero was defined as the point at which the mean force first exceeded 100 N.

The force-time corridor (Figure 3a) of the low energy group produced a higher peak force than Agnew et al. (2024) (1997 N vs. 1685 N). This difference may be attributed to the larger impactor face used in the current study that engaged a greater number of ribs. Despite the higher peak force, peak thoracic deflection was lower in the current study (33.8 mm vs. 39.4 mm, Figure 3b). The larger impactor face distributed the contact force over a wider area and allowed the foam to conform to thorax, avoiding the local loading produced by a smaller rigid impactor. The foam

This paper is a student paper from the 21st Injury Biomechanics Symposium and is published in a special issue of SAE International Journal of Transportation Safety.
It is preliminary work, has not been peer reviewed, and should not be cited because it is a work in progress.

padding may have contributed additionally to limiting localized deflection, though its effect is likely secondary given the relatively small foam deformation observed during impact. Together, these factors produced a stiffer force-deflection response (Figure 3c), with higher measured force but lower localized deflection, suggesting that a larger contact area reduces local stress and limits localized deformation at the chestband level.

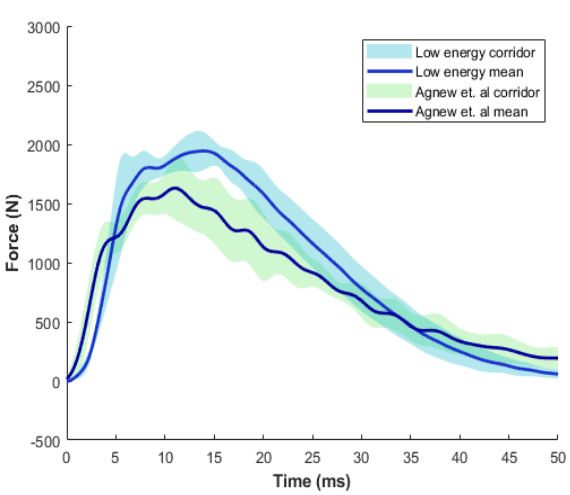

a) Force-time corridors

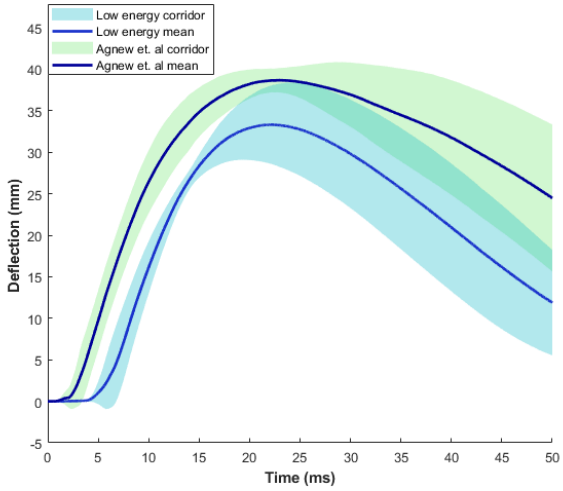

b) Deflection-time corridors

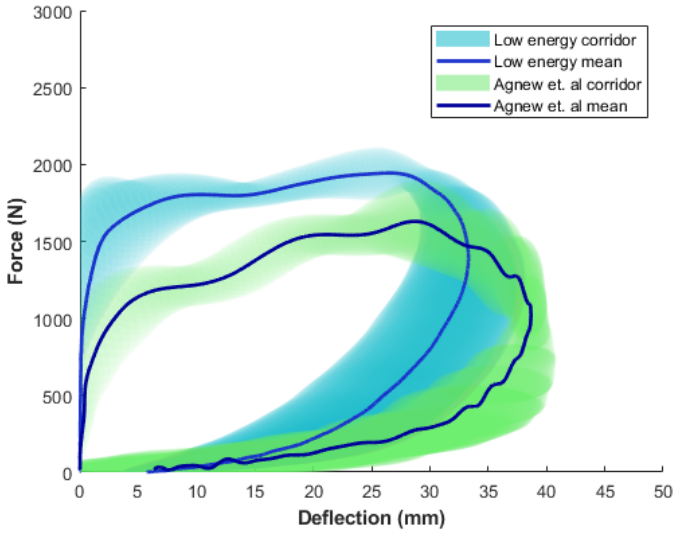

c) Force-deflection corridors

Figure 3: Corridor comparisons for the low energy group from the current study (cyan) vs. Agnew et al. (2024) (green)

This paper is a student paper from the 21st Injury Biomechanics Symposium and is published in a special issue of SAE International Journal of Transportation Safety.
It is preliminary work, has not been peer reviewed, and should not be cited because it is a work in progress.

Bolte et al. (2023) conducted sled tests with realistic boundary conditions on small female PMHS at a higher impact velocity (approximately 14 m/s) and reported a mean percent chest deflection of 14.8 % across test conditions (standard airbag vs c-airbag). In comparison, the current study demonstrated mean percent chest deflections of 12.2 % in the low-energy group and 15.7 % in the high-energy group. This provides a meaningful point of comparison between the current experiment and more realistic sled test conditions and further supports the relevance of the high energy condition to real-world lateral impact scenarios.

The acceleration responses of the thorax (Table 4) were consistent with the impact configuration (Figure 1c). The top of the impactor was positioned closer to T4, and the shape of the thorax resulted in greater contact area engagement at this level. This explains the significantly greater y-axis accelerations observed at T4 in the high energy group. Angular velocity about the x-axis did not differ significantly between groups, indicating that bending about this axis is less sensitive to changes in impact energy. The sternum exhibited greater z-axis angular velocity rotational magnitudes than the thoracic spine. This is consistent with the sternum's reduced anatomical constraint relative to the vertebral column (Figure 4) and supports the presence of twisting during impact.

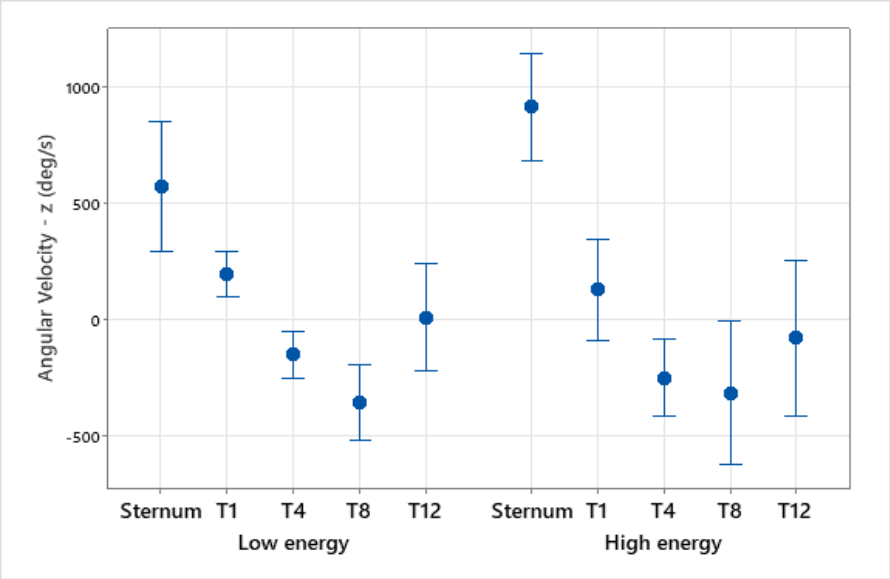

Figure 4: Z-angular velocity of sternum and thoracic spine locations in low and high energy groups. Individual standard deviations were used to calculate intervals.

This paper is a student paper from the 21st Injury Biomechanics Symposium and is published in a special issue of SAE International Journal of Transportation Safety.
It is preliminary work, has not been peer reviewed, and should not be cited because it is a work in progress.

Limitations

This study has several limitations that should be considered when interpreting the findings. The small sample size of six PMHS per energy group limits the statistical power and generalizability of the derived corridors and injury metrics, and future work with larger samples is needed to better resolve subject-specific contributors to thoracic response variability. Small test-to-test variations in impact velocity, while within acceptable limits, may influence peak force. Finally, subject-specific soft tissue properties and thoracic geometry, including rib cortical thickness and chest wall dimensions, were not quantified, limiting the ability to isolate their contributions to the inter-subject variability observed in force and deflection.

CONCLUSIONS

This study provides female-specific thoracic biomechanical response data generated under simplified conditions with realistic components. The results demonstrate that PMHS responses are sensitive to differences in impact energy input, i.e., force, deflection, deformation energy, and kinematic responses increased with increased impact severity. These findings establish an experimental foundation for small female thoracic response and provide valuable data for ATD and HBM validation. Future work will focus on characterizing injury mechanisms and developing improved injury prediction capabilities to enhance occupant protection for female occupants in side impact crashes.

ACKNOWLEDGEMENTS

The authors are incredibly grateful to the anatomical donors who made this research possible. The authors would also like to thank all IBRC personnel for their important contributions to this research.

REFERENCES

AGNEW, A. M., BAKER, G. H., MARCALLINI, A., BENDIG, A., MOORHOUSE, K., RHULE, H., BOLTE, J. H., and KANG, Y. S. Small female post-mortem human subject (PMHS) thoracic responses to simplified oblique and lateral loading. IRC-24-23 IRCOBI Conference Proceedings, 274–291, 2024.

BAKER, G., KANG, Y. S., MARCALLINI, A., LANG, R., HUTTER, E., MOORHOUSE, K., and AGNEW, A. M. Female PMHS thoracic biomechanical response corridors with preliminary consideration of the influence of breast tissue in frontal impacts. Stapp Car Crash J., in press, 2026.

This paper is a student paper from the 21st Injury Biomechanics Symposium and is published in a special issue of SAE International Journal of Transportation Safety.
It is preliminary work, has not been peer reviewed, and should not be cited because it is a work in progress.

BOLTE, J., FIBBI, C., TESNY, A. C., KANG, Y. S., AGNEW, A. M., SHURTZ, B. K., and MOORHOUSE, K. Analysis of injury mechanism and thoracic response of elderly, small female PMHS in near-side impact scenarios. Traffic Inj. Prev. 24(S1): S23–S31, 2023.

BOSE, D., SEGUI-GOMEZ, M., and CRANDALL, J. R. Vulnerability of female drivers involved in motor vehicle crashes: an analysis of US population at risk. Am. J. Public Health 101(12):2368–2373, 2011.

BRUMBELOW, M. L. and JERMAKIAN, J. S. Injury risks and crashworthiness benefits for females and males: which differences are physiological? Traffic Inj. Prev. 23(1):11–16, 2022.

BRUMBELOW, M. L., MUELLER, B. C., and ARBELAEZ, R. A. Occurrence of serious injury in real-world side impacts of vehicles with good side-impact protection ratings. Traffic Inj. Prev. 16(S1): S125–S132, 2015.

CRAIG, M. J., ATWOOD, J. R. E., LIU, C., ZHANG, F., RUDD, R., BENEDETTI, M. H., and ENRIQUEZ, J. Sex-based differences in odds of motor vehicle crash injury outcomes. Report No. DOT HS 813 754. National Highway Traffic Safety Administration, 2026.

DALMOTAS, D., CHOUINARD, A., COMEAU, J. L., GERMAN, A., ROBBINS, G., and PRASAD, P. Examination of crash injury risk as a function of occupant demographics. Stapp Car Crash J. 67:14–33, 2024.

IRWIN, A. L., MERTZ, H. J., ELHAGEDIAB, A. M., and MOSS, S. Guidelines for assessing the biofidelity of side impact dummies of various sizes and ages. Stapp Car Crash J. 46:297–319, 2002.

KANG, Y. S., BENDIG, A., STAMMEN, J., HUTTER, E., MOORHOUSE, K., BOLTE, J. H., and AGNEW, A. M. Comparison of small female PMHS thoracic responses to scaled response corridors in a frontal hub impact. Traffic Inj. Prev. 24(1):62–68, 2023.

KEMPER, A. R., MCNALLY, C., KENNEDY, E. A., MANOOGIAN, S. J., and DUMA, S. M. The influence of arm position on thoracic response in side impacts. Stapp Car Crash J. 52:379–420, 2008.

KROELL, C., SCHNEIDER, D., and NAHUM, A. Impact tolerance and response of the human thorax. 15th Stapp Car Crash Conference, San Diego, CA, 1971.

KROELL, C., SCHNEIDER, D., and NAHUM, A. Impact tolerance and response of the human thorax II. 18th Stapp Car Crash Conference, Ann Arbor, MI, 1974.

MOORHOUSE, K. An improved normalization methodology for developing mean human response curves. International Technical Conference on the Enhanced Safety of Vehicles, Seoul, Korea, 2013.

This paper is a student paper from the 21st Injury Biomechanics Symposium and is published in a special issue of SAE International Journal of Transportation Safety.
It is preliminary work, has not been peer reviewed, and should not be cited because it is a work in progress.

NOH, E. Y., ATWOOD, J., LEE, E., CRAIG, M., and CHEN, C. L. Female crash fatality risk relative to males for similar physical impacts. Report No. DOT HS 813 358. National Highway Traffic Safety Administration, 2022.

NUSHOLTZ, G., MELVIN, J., and LUX, P. The influence of impact energy and direction on thoracic response. 27th Stapp Car Crash Conference, San Diego, CA, 1983.

PRASAD, P., DALMOTAS, D., and CHOUINARD, A. Side impact regulatory trends, crash environment, and injury risk in the USA. Stapp Car Crash J. 59:91–112, 2015.

RHULE, H., SUNTAY, B., HERRIOTT, R., AMENSON, T., STRICKLIN, J., and BOLTE, J. H. Response of PMHS to high- and low-speed oblique and lateral pneumatic ram impacts. Stapp Car Crash J. 55:281–315, 2011.

Safety Test Instrumentation Standards Committee. Instrumentation for impact test — part 1: electronic instrumentation. SAE J211/1. SAE International, 2022.

SHAW, J. M., HERRIOTT, R. G., MCFADDEN, J. D., DONNELLY, B. R., and BOLTE, J. H. Oblique and lateral impact response of the PMHS thorax. Stapp Car Crash J. 50:147–167, 2006.

SLYKHOUSE, L., ZASECK, L. W., MILLER, C., HUMM, J. R., ALAI, A., KANG, Y. S., DOOLEY, C., SHERMAN, D., BIGLER, B., DEMETROPOULOS, C. K., REED, M. P., and RUPP, J. D. Anatomically based skeletal coordinate systems for use with impact biomechanics data intended for anthropomorphic test device development. J. Biomech. 92:162–168, 2019.

YOGANANDAN, N., HUMM, J. R., PINTAR, F. A., and BRASEL, K. Region-specific deflection responses of WorldSID and ES2-re devices in pure lateral and oblique side impacts. Stapp Car Crash J. 55:351–378, 2011.

This paper is a student paper from the 21st Injury Biomechanics Symposium and is published in a special issue of SAE International Journal of Transportation Safety.
It is preliminary work, has not been peer reviewed, and should not be cited because it is a work in progress.